Kochi Chapter

Indian Geotechnical Conference
IGC 2022
15th – 17th December, 2022, Kochi

Numerical Analysis on the Stability of Upstream Mine Tailings Dam under Seismic Loading

Mujeeb Ul Rehman [0000-0001-9414-5195], Saptarshi Kundu [0000-0002-9290-7966] and Dipankana Bhattacherjee [0000-0003-4333-5356]

Department of Civil Engineering, Indian Institute of Engineering Science and Technology, Shibpur, Howrah 711103, India. E-mail:dipankana@civil.iiests.ac.in

Abstract. Upstream tailings dam expedites the construction process while lowering disposal and operational expenses. However, these dams are susceptible to liquefaction-induced failure under seismic conditions. This study explores the possibility of reducing differential settlement of the upstream tailings dam under liquefaction by densifying strategic portions of the beach area. Finite Element analysis is conducted using UBC3D-PLM constitutive law to model the liquefiable soil. The model is validated with a published centrifuge model of clayey embankment resting on liquefiable sand. The vertical deformation and post-liquefaction factor for unimproved and improved upstream tailings dam are numerically analysed. For an unimproved upstream tailings dam, vertical deformation to the tune of 300 mm was observed after 100 seconds of the seismic load, while the post-liquefaction stability factor was 1.33. In order to enhance the stability of the upstream tailings dam, the portion of the beach under the raised embankment was densified at a relative density of 70%. The width and depth of densified portions were varied as a function of beach length. This study suggests a method of improving the stability of the upstream tailings dam under seismic conditions while making the construction procedure of these dams easy and cost-effective.

Keywords: Mine Tailings, Upstream Tailings Dam, Liquefaction, Deformation, Densification, Beach Length.

1 Introduction

Earth has served as the driving force behind the mining industries' pursuit of various minerals and metals with great economic worth. Mining is done to extract the minerals from the ores, producing several thousand million tonnes of waste annually [1], [2]. The growth in modern technology and the rise in living standards have significantly raised the demand for minerals, metals, etc., which has increased the extraction of material from the earth and consequently increased the amount of waste produced. These wastes are primarily made up of tailings, the mixture of ground-up rocks, processed fluids and containments left over after the minerals have been extracted from the ore. Additionally, these tailings range in particle size from coarse to fine, and they have characteristics similar to sand and clayey silt, respectively [3], [4], [5]. Considering the diverse nature of the tailings, disposal is quite challenging. The direct disposal of these tailings can be fatal and destructive for the surrounding environment of the mine. A common and effective method of disposal of these tailings is thus to retain them behind the retaining structure, referred to as a mine tailings dam, which is the topic of interest in this study.

Mine tailings dams are mega structures built with an aim to retain the mine tailings and to reuse the processed water after treating it efficiently. According to the portfolio of World Mine Tailings Failures, there are around 29000 to 35000 mine tailings dam, which retain 534 billion cubic metres of tailings. Tailings are disposed of using the cyclone separator which assures the separation of the coarse and finer fraction of the tailings. The coarser fraction is used for the construction of tailings dam after proper compaction, while the finer fraction is retained behind the tailings. The construction of tailing dams is different from water dams in a sense that, even after the construction of the starter embankment, these are raised to store the increasing quantity of mine tailings. This process thus continues up to the functional life of the mining industry. Based on how the raised embankments are constructed, tailings dam are classified as the upstream, downstream and center line, as represented in Figure 1(a-c).

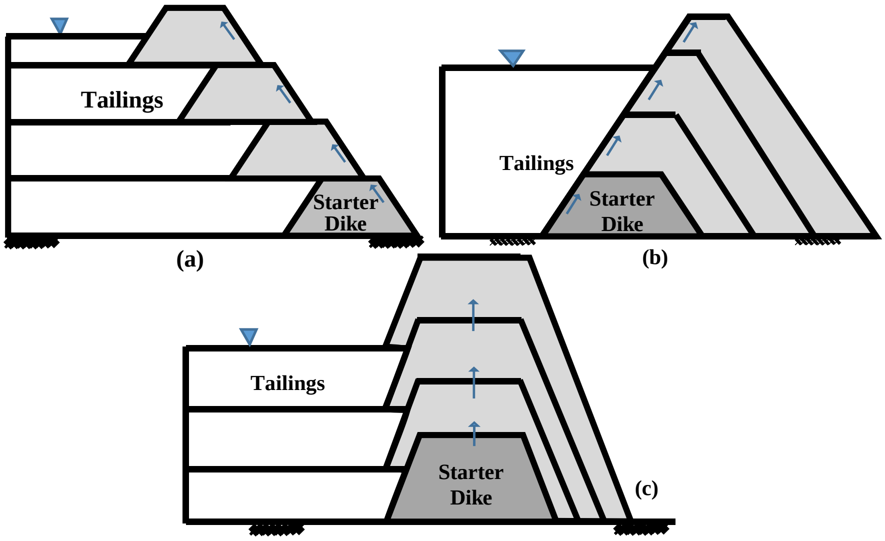

Fig. 1. Classification of tailings dam (a) Upstream (b) Downstream (c) Centerline

At the outset, 'starter dykes' are constructed to store the tailings and to prevent contamination of the surrounding environment. If these dams are not adequately engineered during construction, they experience failure, devastatingly affecting the surroundings, aquatic life, human and animal life, economy, etc. Past has witnessed several tailings dam failures triggered due to seepage, overtopping, foundation failure, and liquefaction induced by seismic loads. Among these causes, failures caused by the liquefaction have contributed to the maximum extent and have provoked other local failures, including piping failure, slope failures, overtopping, etc. Liquefaction is triggered by earthquakes with loss in strength, ensuing in considerable deformity and instability in the tailings dam. In the past, many liquefaction-provoked tailing dam failures were reported. The Cadia tailing dam failure occurred in Australia in 2018, where 1.33 billion cubic meters of tailing was relinquished towards the downside of a dam. Apart from this, Brumadinho tailing dam failure of Brazil in 2019 resulted in 300 fatalities with the release of about 12 million cubic meters of tailings, and it also left a considerable impact on the surrounding environment [6]

In the course of studies about copper silty tailings [7], it was observed that the tailings undergo strain softening under high confining pressures, and the maximum shear strength was achieved at 5% strain. The density of the tailings also influences the liquefaction resistance [7]. It was further inferred that at the same cyclic stress ratio, the vibration time for liquefaction and the resistance against liquefaction rises with an increase in dry density from 14.81 to 15.79 kN/m^3. Centrifuge model tests were conducted on the thickened fine tailing obtained from the copper-gold mine to investigate the consolidation and liquefaction susceptibility of these tailings [8]. It was found that after simulating a seismic excitation having a peak acceleration of 0.20g, a significant drop was measured by the accelerometers embedded in the soil, which indicated that liquefaction had occurred in the mine tailing. Moreover, few acceleration cycles were required to liquefy the tailings present at the shallow depth [8]. A numerical study was also carried out [9] to investigate the liquefaction potential and stability of the Aitik copper tailings dam raised by the upstream method under the dynamic loads. The results displayed that for an earthquake of magnitude 5.8, the liquefied zone occurred near the embankment dyke at a depth of 4m, and for an earthquake of magnitude 3.6, no such zones could be observed. Since the zone of liquefiable tailing was small, so the stability of the dam was not affected [9]. Briefly summarising, even though much research has been done on the liquefaction analysis of tailings and tailing dams, less attention has been given for improving the stability of the mine tailings dam.

Among the three types of the mine tailings dam, the upstream tailings dam is cheap, easy and involves quick construction methodology. However, these dams are prone to failures due to liquefaction. Figure 2 demonstrates failure cases encountered based on the configuration of tailings dam. The raised embankment of the upstream tailing dam resting on the tailings undergoes liquefaction during seismic conditions, which results in the generation of excess pore water pressure, thereby reducing the strength of tailings and leading to differential dam settlement. This minimises the serviceability and functioning of the dam. These dams thus need an attention for improving their stability and serviceability under seismic conditions.

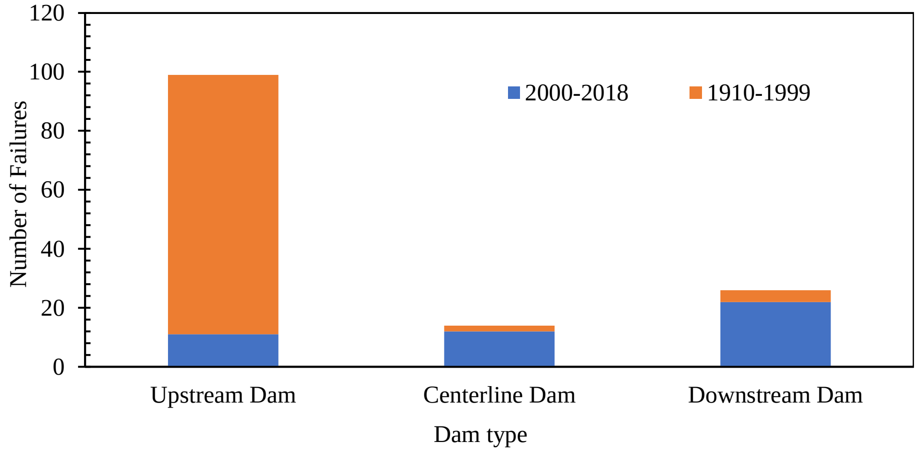

Fig. 2. Failure distribution of mine tailings dam based on dam type [10]

In this study, the behaviour of upstream tailings dam was analysed under seismic conditions using finite element-based software PLAXIS 2D. In order to account for the stability of the upstream tailings dam, the strategic portion of the beach area (region of the tailings pond on which some part of the raised embankment will rest) was improved on which raised embankment is resting. The improved zone was densified to a relative density of 70%, and the influence of the width and depth of the improved zone on the stability of the dam was analysed numerically. The effect of the improvement can be determined by comparing the vertical deformation at strategic points and the factor of safety before and after improvement.

2 Validation of the Developed Numerical Model

For the validation of the developed numerical model, the centrifuge model tests [11] on clayey embankment resting on liquefiable Nevada sand at 75 g was numerically modelled in PLAXIS 2D. The liquefiable Nevada sand and clayey embankment were modelled using UBC3D-PLM and Mohr-Coulomb constitutive laws respectively. Details of the dimensions and boundary conditions of the numerical model are shown in Figure 3 and Figure 4. A finer mesh size is adopted at the interface of the clay embankment and Nevada sand during validation study. The material properties of the clayey embankment and Nevada sand are presented in Table 1 and Table 2 respectively.

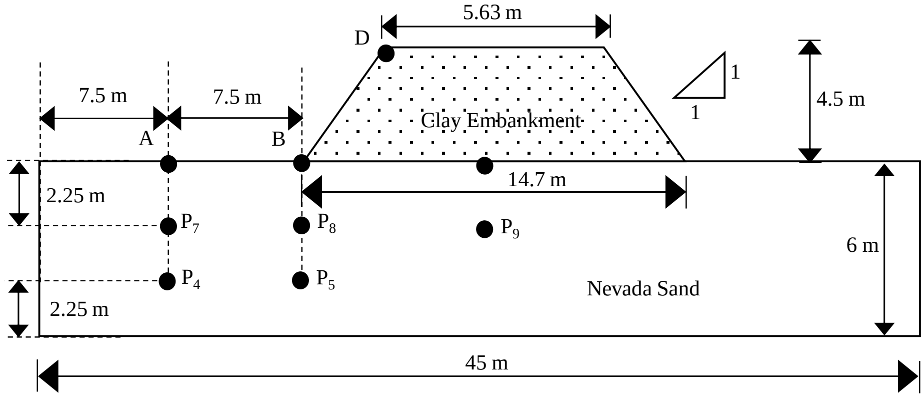

Fig. 3. Dimensions of a numerical model for validation with centrifuge tests [11]

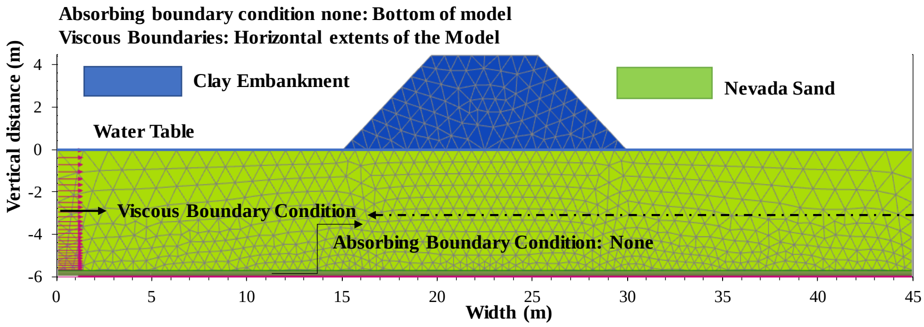

Fig. 4. Finite element mesh and boundary conditions for model prepared in PLAXIS 2D

Table 1. Properties of clayey embankment [12]

Properties	Symbol	Units	Value
Dry Unit Weight	γ_{dry}	kN/m^3	19
Saturated Unit Weight	γ_{sat}	kN/m^3	21
Initial Void Ratio	$e_{initial}$	-	0.5
Cohesion	c	kN/m^2	22
Internal Angle of Friction	ϕ	°	31
Modulus of Elasticity	E	kN/m^2	20,000
Poisson's Ratio	μ	-	0.3
Permeability	k	m/day	0.6

The numerical model simulating the centrifuge experiment was subjected to a cyclic load of 10 cycles of 1.6 Hz with a maximum amplitude of excitation of 0.09g, as presented in Figure 5. The excess pore water pressure (Excess PWP) was computed at strategic points and the results were compared at homologous points with the centrifuge model, as depicted in Figure 6, Figure 7 and Figure 8. It was observed that the time at which peak excess pore water pressure was observed at a particular point in the dam section corroborated numerically and experimentally. Moreover, the initial rise in excess pore-water pressure was similar in both models. However, the rate of dissipation of excess pore water pressure was higher in the numerical model than in the centrifuge model.

Table 2. UBC3D-PLM Parameters of Nevada Sand [12]

Parameter	Symbol	Units	Value
Dry Unit Weight	γ_{dry}	kN/m^3	16.60
Saturated Unit Weight	γ_{sat}	kN/m^3	19.64
Initial Void Ratio	$e_{initial}$	-	0.763
Permeability	$[k_x = k_y = k_z]$	m/day	47.52
Elastic shear modulus number	K_G^e	-	809.4
Elastic Bulk modulus number	K_B^e	-	566.6
Plastic shear modulus number	K_G^p	-	202.6
Elastic shear modulus index	*ne*	-	0.5
Elastic Bulk modulus index	*me*	-	0.5
Plastic shear modulus index	*np*	-	0.4
Atmospheric Pressure	P_a	kPa	100
Constant volume friction angle	ϕ_{cv}	°	33
Peak friction angle	ϕ_p	°	33.65
Cohesion	*C*	kPa	-
Tension cut-off	σ_t	kPa	0.0
Failure Ratio	R_f	-	0.83
SPT-N Values	$(N_1)_{60}$	-	6.5
Densification factor	f_{achard}	-	0.45
Post Liquefaction Factor	f_{acpost}	-	0.02

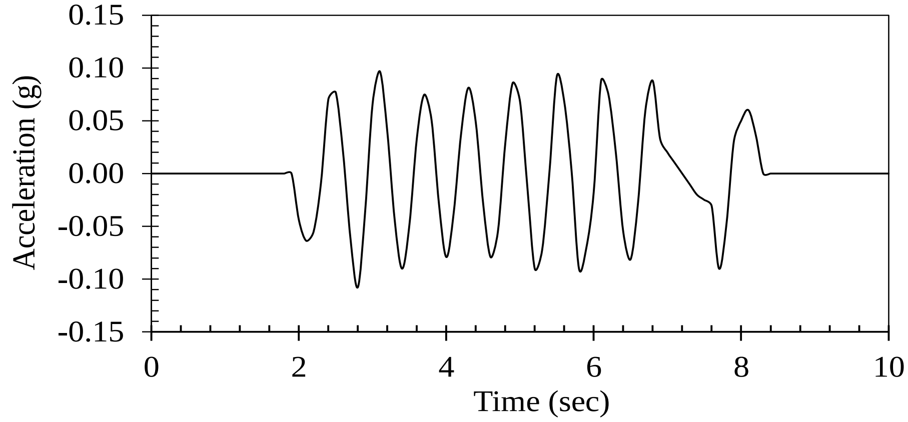

Fig. 5. Input motion provided at the base of the numerical model [11]

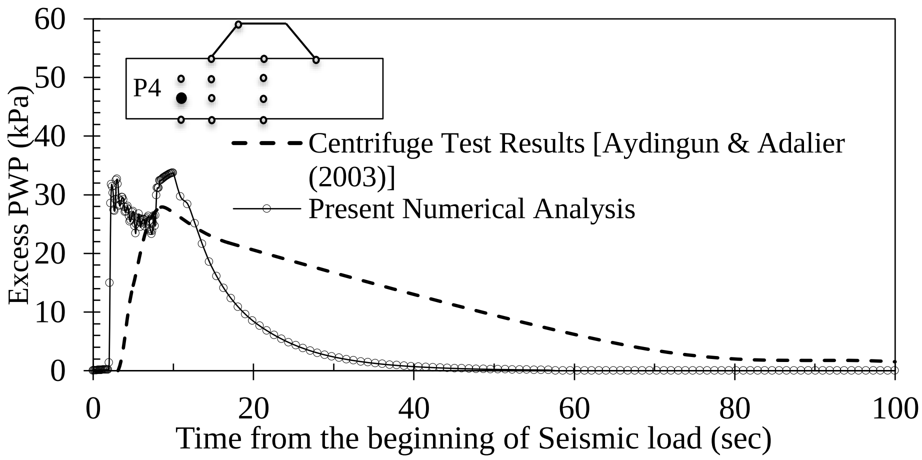

Fig. 6. Comparison of excess pore water pressure (PWP) between the centrifuge and numerical model

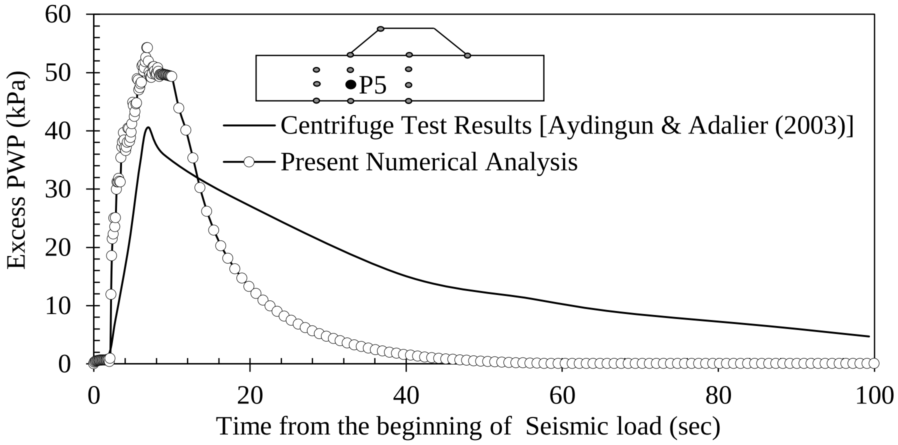

Fig. 7. Comparison of excess PWP between the centrifuge and numerical model

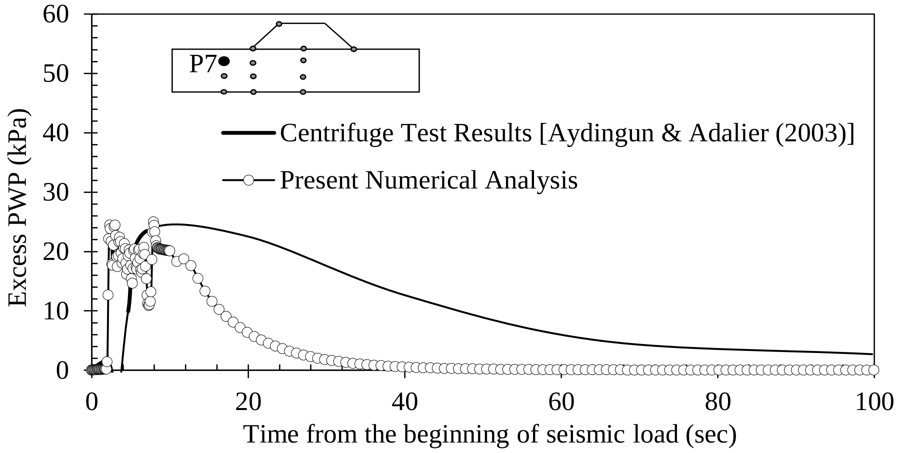

Fig. 8. Comparison of excess PWP between the centrifuge and numerical model

3 Numerical Modelling of Upstream Tailings Dam

After the validation of the numerical mode, an upstream tailings dam was modelled numerically using 15 noded triangular elements and assuming plain strain conditions. The total height of the dam was kept at 14 m retaining 12.5 m high tailings with a phreatic level coinciding with the tailing level. The raised embankment was 4 m in height with a side slope of 1 vertical: and 2 horizontal. The initial embankment of height 10 m was provided with a drainage blanket of 0.5 m thickness and 23 m width, and the entire dam structure rested on a 10 m deep rock foundation. UBC3D-PLM soil constitutive model was used to predict the liquefaction and post-liquefaction behaviour of the tailing and tailings dam. In this study, a relatively coarse mesh was used for modelling the foundation material of the upstream dam, while a fine mesh was used for modelling the tailings, dam body and improved zones, as shown in Fig. 9.

Figure 9 represents the numerical model of the upstream dam without improvement. The improved zone was taken into account to analyse its influence on the behaviour of the dam under seismic conditions as shown in Figure 10. The dam was subjected to the same cyclic load which was used during validation. The width and depth of the improved zone were varied as a fraction of the beach length, Lo (a portion of raised embankment resting on the tailings pond) and their influence of the behaviour of the dam was studied. The improved zone was considered to be compacted at 70%

relative density, with length (mLo) and depth (nLo)] varying as a function of beach length. Here, "m" represents the ratio of the depth of the improved zone to beach length and "n" represents the ratio of the width of an improved zone to beach length. Vertical deformation at salient dam locations was compared before and after improvement. Moreover, the factor of safety of the upstream tailings dam before and after improvement was compared to determine the effectiveness of the ground improvement. Table 3 and Table 4 summarize the properties of the upstream tailings dam and improved zone respectively.4

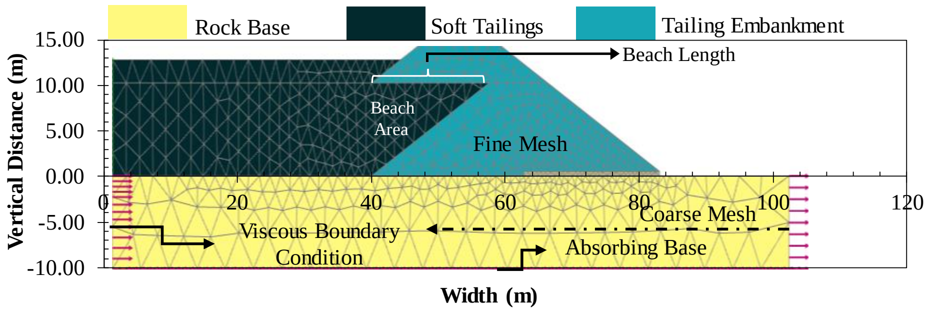

Fig. 9. Numerical model of upstream tailings dam without improvement

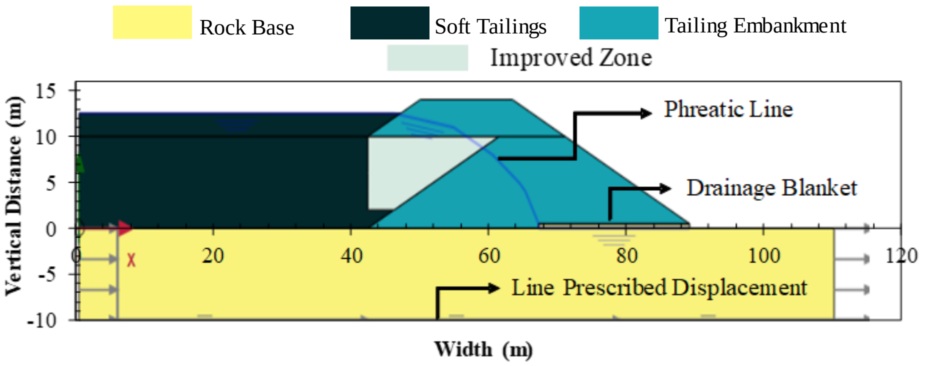

Fig. 10. Numerical model of upstream tailings dam after improvement

4 Results and Discussion

4.1 Vertical Deformation at different dam locations

Vertical deformations at salient points B (mid-point of the raised embankment top surface), C (crest of the raised embankment) and E (mid-depth of the raised embankment) were analyzed in both improved and unimproved dams and have been presented in Figure 11, Figure 12 and Figure 13. It was found that initially in the unimproved dam, the vertical deformation at B, C and E were 209 mm, 300 mm, and 297 mm. The large magnitude of settlement at these points is attributed primarily to the fact that the portion of the tailings supporting the raised embankment undergoes liquefaction, thereby causing a significant reduction in strength and stiffness. This reduction in strength causes the raised embankment to undergo substantial settlement. It was further observed that the vertical deformation decreases with the increase in the width and depth of the improved zone. The least vertical deformation was observed when the depth of the improved zone was 0.5 times the beach length. It was also observed that beyond the case of improved zones of width 1.2 times the beach length, the vertical deformations remained almost constant.

Table 3. UBC3D-PLM parameters for densified tailings

Properties	Units	Unimproved tailings	Densified tailings
Relative Density	-	38	70
Correct SPT value	-	6	20.09
Correct SPT value (Rounded)	-	6	20
Specific Gravity	-	-	2.7
Maximum Void Ratio	-	-	0.75
Minimum Void Ratio	-	-	0.55
Void ratio	-	0.5	0.61
Dry unit weight	kN/m^3	18	16.45
Saturated unit weight	kN/m^3	18	20.17
Elastic shear modulus number	-	120	1176.88
Elastic bulk modulus number	-	120	823.82
Plastic shear modulus number	-	36	1512.23
Peak friction angle	°	18.6	37.55
constant volume friction angle	°	18	34.55
Permeability	m/s	1.00E-05	1.00E-04
Failure ratio	-	0.95	0.72
Post liquefaction factor	-	0.3	0.2
Densification factor	-	0.1	1
Elastic shear modulus index	-	0.5	0.5
Elastic bulk modulus index	-	0.5	0.5
Plastic shear modulus index	-	0.4	0.4
Cohesion	kN/m^2	1	1

Table 4. Material properties of different sections of upstream tailings dam

Properties	Tailing Layer	Dam Material	Rock Base
Model	UBC3D-PLM	UBC3D-PLM	Linear Elastic
Relative Density	38	80	-
Correct SPT value	6	26.24	-
Correct SPT value (Rounded)	6	26	-
Specific Gravity	-	-	-
Maximum Void Ratio	-	-	-
Minimum Void Ratio	-	-	-
Void ratio	-	-	-
Dry unit weight (kN/m^3)	18	16.66	26
Saturated unit weight (kN/m^3)	18	20.31	26
Elastic shear modulus number	120	1284.32	-
Elastic bulk modulus number	120	899.03	-
Plastic shear modulus number	36	2704.62	-
Peak friction angle (°)	18.6	40.01	-
Constant volume friction angle (°)	18	35.21	-
Permeability (m/s)	1.00E-05	1.00E-07	0
Failure ratio	0.95	0.67	-
Post liquefaction factor	0.3	0.2	-
Densification factor	0.1	1	-
Elastic shear modulus index	0.5	0.5	-
Elastic bulk modulus index	0.5	0.5	-
Plastic shear modulus index	0.4	0.4	-
Friction Angle	-	-	-
Cohesion (kN/m^2)	1	13	3500
Poissons Ratio	0.12	0.12	0.25
Modulus of Elasticity (kN/m^2)	3000	7200	35500000
Reference	[9]	[9]	[13]

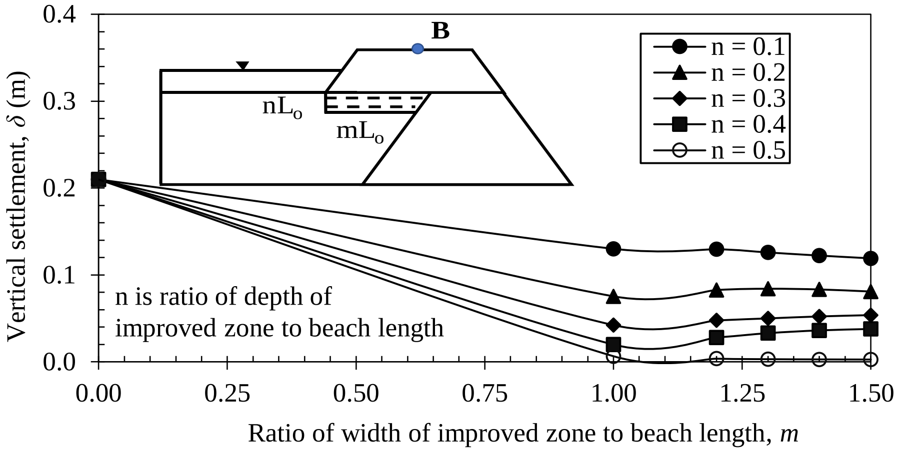

Fig. 11. Vertical deformation at point B after 100 seconds from the beginning of the seismic load

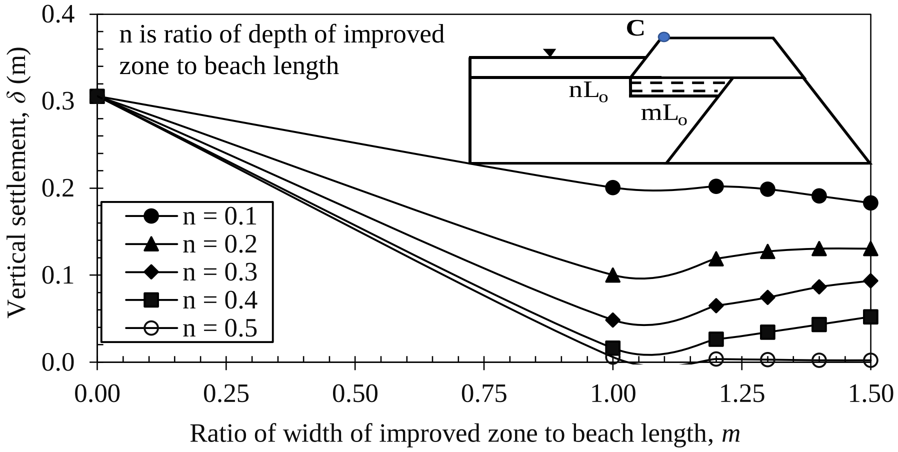

Fig. 12. Vertical deformation at point C after 100 seconds from the beginning of the seismic load

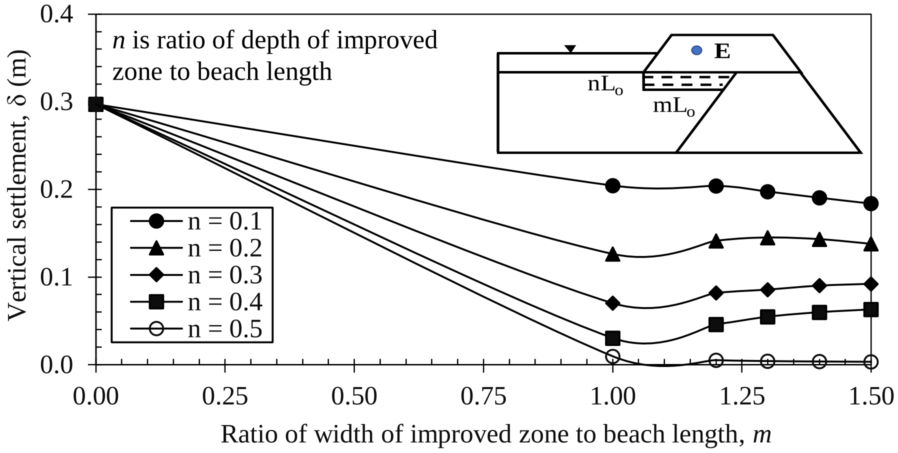

Fig. 13. Vertical deformation at point E after 100 seconds from the beginning of the seismic load

4.2 Factor of Safety

Post liquefaction factor of safety was obtained from the numerical analysis for both the unimproved and improved upstream tailings dam. It was found that the factor of safety increases from 1.33 to 1.687 with the inclusion of the improved zone. In general, the factor of safety was observed to increase with an increase in the depth and width of the improved zone. A factor of safety exceeding 1.45 was obtained for the width of the improved zone greater than 1.2 times the beach length and for depth greater than 0.2 times the beach length. It was observed that a maximum factor of safety of 1.687 was obtained when the depth of the improved zone was 0.5 times the beach length and the width was 0.5 times the beach length. The variation of the factor of safety with the width and depth of the improved zone has been presented in Figure 14.

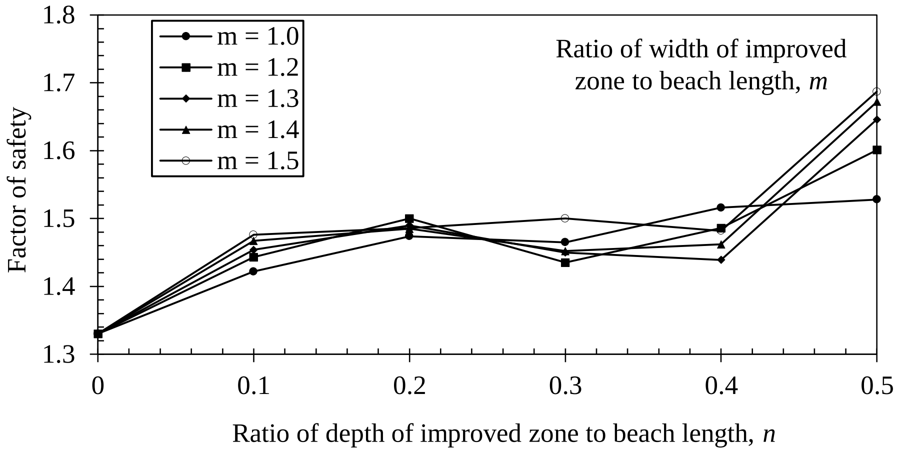

Fig. 14 Variation of factor of safety of dam

5 Conclusion

An upstream tailings dam was modelled in this study numerically in PLAXIS 2D interface to study the response under seismic loading. Initially, the dam was found to undergo liquefaction-induced failure resulting in excessive differential settlement and instability. In order to improve its stability, the strategic zone under the raised embankment of the dam was modelled with soil material properties representing densified tailings and made to achieve a relative density of 70%. The vertical deformation at different dam locations and factor of safety was compared to determine the effectiveness of the improvement. The major conclusion that can be drawn from the study are as follows:

1) This study proposes a strategy for improving the stability of the upstream tailings dam under seismic circumstances while making the construction method of these dams simple and economic. Densification was found effective in enhancing the stability of the upstream tailings dam under seismic conditions.
2) The vertical deformation at different dam locations was observed to reduce significantly with the increase in the depth and width of the improved zone. The least vertical deformation occurred at a depth of 0.5 times the beach length and a width of 1.5 times the beach length.
3) The optimum width of improvement for 70% relative density was found to be 1.2 times the beach length and the optimum depth of improvement was found to be

in the range of 0.3 – 0.5 times the beach length. Hence, the depth of the improvement will depend on the cost and importance of the project.

4) The factor of safety was found to increase from 1.33 to 1.687 owing to strategic densification of the portion of the beach area on which the raised embankment is resting. The factor of safety was found to exceed 1.45 for the depth of the improved zone greater than 1.2 times the beach length and the width of the improved zone greater than 0.2 times the beach length.
5) The maximum factor of safety of 1.687 was obtained for an improved zone of depth and width 0.5 and 1.5 times the beach length respectively.
6) This numerical study will help the site engineers to get an insight into the depth and width of the improved zone to be implemented in the field for maintaining the stability of the upstream tailings dam under seismicity.

The results thus highlight that upon the inclusion of the densified region in the tailings pond under the raised embankment, the differential settlement reduces by a significant proportion. Hence, this study offers a workable solution for making upstream tailings dams more stable during seismic conditions while also making the process of building these dams quick and affordable. The study can be further extended by considering the influence of unsaturation, sloping tailing layers, age of tailings, high and partial saturation levels, drainage, foundation material, heterogeneity etc. on the seismic behaviour of the tailings dam.

References

[1] Fourie, A. B., Blight, G. E., Papageorgiou, G.: Static liquefaction as a possible explanation for the Merriespruit tailings dam failure: Reply. Canadian Geotechnical Journal 39(6), 1441-1442 (2002) doi: 10.1139/t02-079.

[2] Fyfe, W. S.: The environmental crisis: Quantifying geosphere interactions. Science, 213, no. 4503, 105-110 (1981) doi: 10.1126/science.213.4503.105.

[3] Ishihara, K.: Post-earthquake failure of a tailings dam due to liquefaction of the pond deposit. First International Conference on Case Histories in Geotechnical Engineering, University of Missouri-Rolla, vol 3, 1129-1143 (1984).

[4] James, M., Aubertin, M., Wijewickreme, D., Wilson, G. W.: A laboratory investigation of the dynamic properties of tailings. Canadian Geotechnical Journal, 48(11), 1587-1600 (2011) doi: 10.1139/t11-060.

[5] Hu, L., Wu, H., Zhang, L., Zhang, P., and Wen, Q.: Geotechnical Properties of Mine Tailings. Journal of Materials in Civil Engineering, 29(2), 04016220 (2017), doi: 10.1061/(asce)mt.1943-5533.0001736.

[6] Davies, M. P.: Tailings Impoundment Failures: Are Geotechnical Engineers Listening? Geotechnical News, 20, 31-36 (2002).

[7] Ming Liu, H., He Yang, C., Zhang, C., Jun Mao, H.: Study on static and dynamic strength characteristics of tailings silty sand and its engineering application. Safety Science, 50(4), pp. 828-834, (2012), doi: 10.1016/j.ssci.2011.08.025.

[8] Antonaki, N., Abdoun, T., Sasanakul, I.: Centrifuge tests on liquefaction potential and slope stability of mine tailings. International Journal of Physical Modelling in Geotechnics, 19(2), 104-114 (2019), doi: 10.1680/jphmg.17.00068.

[9] Zardari, M. A., Mattsson, H., Knutsson, S., Khalid, M. S., Ask, M. V. S., Lund, B.: Numerical analyses of earthquake induced liquefaction and deformation behaviour of an upstream tailings dam. Advances in Materials Science and Engineering, vol. 2017 (2017) doi: 10.1155/2017/5389308.

[10] D. Kossoff, W. E. Dubbin, M. Alfredsson, S. J. Edwards, M. G. Macklin, K. A. Hudson-Edwards: Mine tailings dams: Characteristics, failure, environmental impacts, and remediation. Applied Geochemistry, 51, 229-245 (2014), doi: 10.1016/j.apgeochem.2014.09.010.

[11] O. Aydingun, K. Adalier: Numerical analysis of seismically induced liquefaction in earth embankment foundations. Part I. Benchmark model. Canadian Geotechnical Journal, 40(4), 753-765, (2003), doi: 10.1139/T03-025.

[12] Bhatnagar, S., Kumari, S., and Sawant, V. A.: Numerical Analysis of Earth Embankment Resting on Liquefiable Soil and Remedial Measures. International Journal of Geomechanics, 16(1), 04015029-1-13, (2016), doi: 10.1061/(ASCE)GM.1943-5622.0000501.

[13] Psarropoulos, P. N., and Tsompanakis, Y.: Stability of tailings dams under static and seismic loading, Canadian Geotechnical Journal, 45(5), 663-675, (2008) doi: 10.1139/T08- 014.

[14] Aljanabi, Q. A., Chik, Z., and Kasa, A.: Construction of a New Highway Embankment on the Soft Clay Soil Treatment by Stone Column in Malaysia. Journal of Engineering Science and Technology, 8(4), 448-456 (2013).